A combined targeted/untargeted LC-MS/MS-based screening approach for mammalian cell lines treated with ionic liquids : Toxicity correlates with metabolic profile

Sanwald, Corinna

Elsevier B.V.
2019-05-15

Sanwald, C, Robciuc, A, Ruokonen, S-K, Wiedmer, S K & Lammerhofer, M 2019, 'A combined targeted/untargeted LC-MS/MS-based screening approach for mammalian cell lines treated with ionic liquids : Toxicity correlates with metabolic profile', Talanta, vol. 197, pp. 472-481. https://doi.org/10.1016/j.talanta.2019.01.054

http://hdl.handle.net/10138/310542
10.1016/j.talanta.2019.01.054

Author's Accepted Manuscript

www.elsevier.com/locate/talanta

A combined Targeted/Untargeted LC-MS/MS-based Screening Approach for Mammalian Cell Lines Treated with Ionic Liquids: Toxicity Correlates with Metabolic Profile

Corinna Sanwald, Alexandra Robciuc, Suvi-Katriina Ruokonen, Susanne K. Wiedmer, Michael Lämmerhofer

PII: S0039-9140(19)30055-4
DOI: https://doi.org/10.1016/j.talanta.2019.01.054
Reference: TAL19505

To appear in: *Talanta*

Received date: 14 December 2018
Revised date: 10 January 2019
Accepted date: 14 January 2019

Cite this article as: Corinna Sanwald, Alexandra Robciuc, Suvi-Katriina Ruokonen, Susanne K. Wiedmer and Michael Lämmerhofer, A combined Targeted/Untargeted LC-MS/MS-based Screening Approach for Mammalian Cell Lines Treated with Ionic Liquids: Toxicity Correlates with Metabolic Profile, *Talanta,* https://doi.org/10.1016/j.talanta.2019.01.054

A combined Targeted/Untargeted LC-MS/MS-based Screening Approach for Mammalian Cell Lines Treated with Ionic Liquids: Toxicity Correlates with Metabolic Profile

Corinna Sanwald[a], Alexandra Robciuc[b], Suvi-Katriina Ruokonen[c], Susanne K. Wiedmer[c]*, Michael Lämmerhofer[a]*

[a]Institute of Pharmaceutical Sciences, Pharmaceutical (Bio-)Analysis, University of Tübingen, Auf der Morgenstelle 8, 72076 Tübingen, Germany

[b]Helsinki Eye Lab, Helsinki University Central Hospital, Biomedicum 1, Haartmaninkatu 8, FI-00290 Helsinki, Finland

[c]Department of Chemistry, University of Helsinki, A. I. Virtasen Aukio 1, Post Office Box 55, FIN-00014 University of Helsinki, Finland

Corinna.Sanwald@uni-tuebingen.de

alexandra.robciuc@helsinki.fi

Suvi.k.ruokonen@gmail.com

susanne.wiedmer@helsinki.fi

michael.laemmerhofer@uni-tuebingen.de

*Authors for correspondence: Department of Chemistry, University of Helsinki, A. I. Virtasen Aukio 1, Post Office Box 55, FIN-00014 University of Helsinki, Finland

*Authors for correspondence: Pharmaceutical (Bio-)Analysis, Institute of Pharmaceutical Sciences, University of Tübingen, Auf der Morgenstelle 8, 72076 Tübingen, Germany, Tel.: +49 7071 29 78793; fax +49 7071 29 4565

Abstract

This work presents the development and validation of a quantitative HILIC UHPLC-ESI-QTOF-MS/MS method for amino acids combined with untargeted metabolic profiling of human corneal epithelial (HCE) cells after treatment with ionic liquids. The work included a preliminary metabotoxicity screening of 14 different ionic liquids, of which 9 carefully selected ionic liquids were chosen for a metabolomics study. This study is focused on the correlation between the toxicity of the ionic liquids and their metabolic profiles. The method development included the comparison of different MS/MS acquisition modes. A sequential window acquisition of all theoretical fragment ion mass spectra (SWATH) method with variable Q1 window widths and narrow Q1 target windows of 5 Da for most of the amino acids was selected as the optimal acquisition mode. Due to the absence of a true blank matrix, ^{13}C,^{15}N-isotopically labelled amino acids were utilized as surrogate calibrants, instead of proteinogenic amino acids. Partial least squares (PLS) analysis of the median effective concentrations (EC_{50}) of 9 selected ionic liquids showed a correlation with their metabolic profile measured by the untargeted screening.

Graphical Abstract:

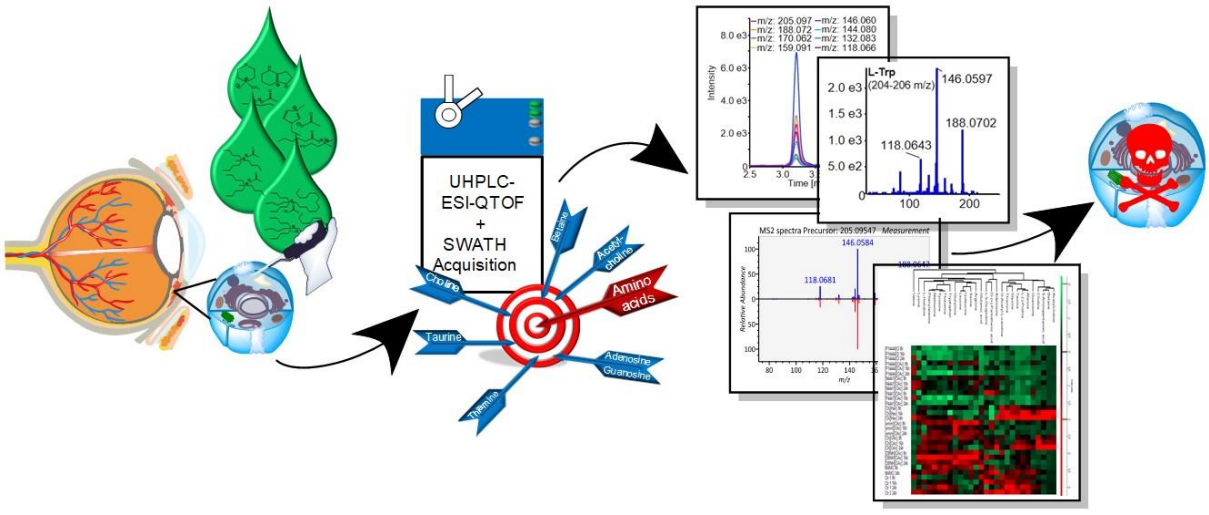

Keywords

Targeted metabolomics, untargeted metabolomics, data-independent acquisition, ionic liquids, toxicometabolomics, human corneal epithelial cells

1. Introduction

The industrial use of ionic liquids (ILs) as environmentally friendly solvents is steadily increasing [1,2]. Because of their structure, ILs are also called “molten salts” [3]. They have many unique characteristics, such as i) wide temperature range (incl. room temperature) of liquid state, ii) thermal, chemical and electrochemical stability, iii) high electrochemical conductivity. Since they are non-flammable, non-explosive, and non-volatile, they are used in many applications, also owing to their large range of solubilities and miscibilities. Their lack of biodegradability, however, renders toxicity studies imperative [4,5]. This matter is complicated because of the high structural variability and large number of existing ILs, requiring a differentiated picture of toxic effects of ILs [1,6,7]. One important future aspect is the structural design and development of environmentally friendly ILs. For this purpose, the understanding of toxic effects is of high importance, and effects of ILs on metabolic profiles might well serve as an indicator for their toxicity. Along this line, toxicometabolomics and toxicolipidomics could shed some light on effects of ILs [8,9].

Such metabolomics studies could be either devised as targeted or untargeted assays. The former make typically use of UHPLC hyphenated to triple quadrupole instruments with electrospray ionization (UHPLC-ESI-QqQ) which has advantages in terms of sensitivity and linear range [9,10]. The latter use high-resolution mass spectrometry (HRMS) hyphenated to UHPLC and allow comprehensive recording of all detectable metabolites. However, the new generation of high-resolution mass spectrometers (QTOF and quadrupole-orbitraps) show improved performance for quantitative analysis [11,12]. Hence, there is an increasing interest in performing qualitative and quantitative analysis in a single run [11,13–16]. In general, HRMS-based untargeted metabolomics is typically performed by data-dependent acquisition

(DDA) (also called information-dependent acquisition, IDA). DDA methods use information from an MS scan for selection of the most abundant precursors for fragmentation being able to identify metabolites based on MS/MS spectra. Unfortunately, low abundant metabolites are not triggered for fragmentation [11,13,17–20]. Relative quantification is exclusively based on MS data which may be less sensitive. To overcome this shortcoming, data-independent acquisition (DIA) such as all-ion fragmentation (AIF), MS^E, or MS/ MS^{ALL} has been proposed as an alternative [20,21]. This acquisition mode selects all precursor ions for simultaneous co-fragmentation. The resultant MS/MS spectra may be relatively complex composite spectra, if many compounds coelute [11,21]. Consequently, qualitative analysis of unknowns may be quite challenging by these classical DIA methods [20,22]. It has been shown that a better spectral quality data can be obtained with a DIA method called sequential window acquisition of all theoretical fragment ion mass spectra (SWATH) [17,19], an acquisition approach first proposed for linear ion trap [23]. In DIA with SWATH, a sequence of MS/MS experiments with intermediate wide Q1 precursor ion selection windows (SWATH windows) (typically 20-30 Da wide) are consecutively stepped through the targeted m/z range [11,22]. The resultant MS/MS spectra are less complex than in AIF or MS^E, which facilitates identification. A broader metabolite coverage compared to DDA was reported [24,25]. Since MS/MS data have been collected comprehensively throughout the chromatogram, quantitative analysis can be performed on the MS/MS level as well, potentially leading to better sensitivity [23].

Amino acids are central cellular metabolites. For instance, they are important for protein synthesis, cell signalling, and redox balance [26]. Major perturbations may indicate problems with cellular homeostasis. Thus, in the current study amino acids were selected as surrogate biomarkers of cellular toxicity of ILs. Numerous HPLC-MS assays for targeted analysis of amino acids have been reported [27–29]. Many times, amino acids were derivatized prior to their analysis to improve detection sensitivity [30]. In the present work, the aim was to develop a fast and straightforward UHPLC-ESI-QTOF-MS/MS method which combines targeted analysis of amino acids without any derivatization and simultaneously allow

untargeted profiling of alterations in the metabolome. DIA with SWATH was used as the acquisition mode to realize this combined qualitative/quantitative assay. Human corneal epithelial (HCE) cells were employed as representative model cells. A wide variety of ILs were selected and the metabolic profiles measured after incubation of the HCE cells with ILs at concentration levels corresponding to their median effective concentration (EC_{50}) values [4]. Here we will demonstrate that there is a correlation between the changes in the metabolic profiles and the toxicity of the ILs.

2. Materials and methods

2.1. Materials and instruments

Ultra-LC-MS grade acetonitrile was purchased from Carl Roth (Karlsruhe, Germany), MilliQ water was purified with an Elga PurLab Ultra purification system (Celle, Germany), ammonium formate was purchased from Sigma Aldrich (Munich, Germany), cell free amino acid mix (20AA, U-13C, 97-99%+; U-15N, 97-99%) and Metabolomics Amino Acid Mix Standard was purchased from Cambridge Isotope Laboratories (Tewksbury, MA ,USA). $^{13}C_2$-maleic acid and $^{13}C_6$-glucose were purchased from Santa Cruz Biotechnology (Heidelberg, Germany), d8-L-valine, ring-d4-L-tyrosine, 3,3,4,4,5,5,6,6-d8-L-lysine·2HCl were purchased from Eurisotop (Saarbrücken, Germany). Phosphate buffered saline (PBS) was made “in-house” by the National Institute of Health and Welfare (THL), Helsinki, Finland. Ham’s F12/Dulbecco’s modified eagle medium (DMEM), fetal bovine serum (FBS), human epidermal growth factor (EGF), insulin, and gentamicin were all purchased from Thermo-Fisher Scientific (Waltham, MA, USA). Methanol and cholera toxin were purchased from Sigma (St. Louis, MO, USA). Cell incubator and centrifuges were from Thermo-Fisher Scientific (Waltham, MA, USA). Samples were ultrasonicated using Soniprep 150 from MSE (London, UK). Standard solutions were prepared as described in Suppl. Material.

2.2. Cell culture and metabolite extraction

The SV-40 immortalized HCE cells [31] were grown in a 10cm petri dish until confluence (8.8 x 10^6 cells) in Ham's F12/DMEM supplemented with 15% FBS and EGF, insulin, cholera toxin and gentamicin. Before IL treatment, the cells were starved for 18 hours in serum free Ham's F12/DMEM supplemented with EGF, insulin, cholera toxin, and gentamicin to achieve serum free conditions, eliminate serum growth factor and nutrient activities on the surface of the cells, and equalize all cells to the same cell cycle phase by stopping the cell growth. After starvation, the cells were incubated with different ILs (Figure 1) dissolved in serum free media to achieve concentrations around their EC_{50} values, determined by Ruokonen *et al.* [4]. After 8, 16, and 24h the petri dishes were placed directly on ice for quenching the enzyme activity immediately. The cell monolayer was washed twice with 5 to 7 mL cold PBS buffer before 600 µL of ice-cold extraction mix was added. The extraction mix composed of 258 µL of MeOH, 300 µL of cell free amino acid mix (1 mg/mL), and 42 µL of ACN:H_2O (1:1 v/v). Next, the cells were scraped from the petri dish wall into the extraction mixture and the suspension of the cells was transferred into an Eppendorf tube. The suspension was ultrasonicated with a MSE Soniprep 150 probe ultrasonicator (10 sec, 23 MHz, pulse of 5-7 microns) and centrifuged at 10 000 g for 5 minutes, and the supernatant separated from the cell pellet was stored at -80 °C until further analysis.

2.3. LC-MS/MS instrumentation

All analyses were performed on a Sciex TripleTOF 5600+ equipped with a Duospray ion source (Sciex, Concord, Ontario; Canada) and carried out with electrospray ionization (ESI) in positive ion mode. The mass spectrometer was coupled to an Agilent 1290 Series UHPLC instrument (Agilent, Waldbronn, Germany) with a Pal HTC-XS autosampler from CTC (Zwingen, Switzerland).

The chromatographic HILIC separation was performed on an Acquity UPLC BEH Amide column (2.1 x 50 mm) packed with 1.7 µm particles (Waters, Eschborn) equipped with an Acquity UPLC BEH Amide 1.7 µm Van-guard column. The mobile phase composed of A) 10 mM ammonium formate in MilliQ water with 0.15 % (v/v) formic acid adjusted to pH 3 and B)

2 mM ammonium formate in ACN with 0.15 % (v/v) formic acid. The following mobile phase gradient was used: 0.00 – 0.50 min, 95 % B; 0.50 – 0.51 min, 95 – 90 % B; 0.51 – 8.00 min, 90 – 70 % B; 8.00 – 10.00 min, 70 % B; 10.00 – 10.01 min, 70 – 95 % B; 10.01 – 12.00 min, 95 % B. The flow rate was 300 µL/min and the column temperature was set at 40 °C. The injection volume was 2 µL for all measurements.

The following MS settings of the mass spectrometer were identical for all four investigated acquisition modes: Curtain gas (CUR) 20 psi, nebulizer gas (GS1) 60 psi, drying gas (GS2) 60 psi, ion-spray voltage floating (ISVF) +4000 V and source temperature (T) 500 °C. Nitrogen was used as curtain gas, nebulizer gas and drying gas.

High-resolution MS and high-sensitivity MS/MS data for the amino acid mixture containing all 20 proteinogenic amino acids, were acquired by three different acquisition modes: MRM^{HR}, SWATH with fixed Q1 window widths and SWATH with variable Q1 window widths (SWATH 2.0) (for details see Suppl. Material). An external calibration was performed every five samples.

For the finally used method, SWATH acquisition mode with variable window widths was utilized. It consisted of a TOF-MS scan (collision energy CE 10 V, declustering potential DP 30 V, cycle time CT 1.3 s, accumulation time AT 200 ms, SW m/z 30–1000 and RF m/z 20 33 %, m/z 70 33 %, m/z 270 34 %) and several different product ion scans with individual CE and DP settings (Table 1). The product ion scans consisted of 27 Q1 windows with different window widths in the mass range of 30–300 m/z (Table 1).

2.4. Calibration and validation

2.4.1. Matrix effect

The matrix effect (ME) can be determined by calculating the ratios of slopes of calibration functions in presence and absence of matrix components, *i.e.* post-extraction spike of surrogate calibrants and neat standard solution of surrogate calibrants, according to eq. 1.

$$ME = \frac{slope_{HCE\ extract}}{slope_{neat\ solution}} * 100 \quad \text{(eq. 1)}$$

Therefore, the $^{13}C,^{15}N$-isotopically labelled amino acids were diluted with ACN:MilliQ water (1:1; v:v) to achieve the same dilutions as described in SI 4. Response factors. The same serial dilutions were prepared in a HCE cell extract (not treated with ILs). Deuterated amino acids were used as internal standards.

2.4.2. Calibration

$^{13}C,^{15}N$-L-amino acids were used as surrogate calibrants for calibration and validation. The surrogate calibration was prepared in a matrix-matched manner. Different amounts of $^{13}C,^{15}N$-amino acid standard mixture were spiked into an untreated HCE cell extract to prepare dilutions of 1:10; 1:20; 1:40; 1:160; 1:640; 1:1000; 1:4000; 1:16 000; 1:64 000 and 1:250 000. The HCE extract itself was finally diluted by a factor of 10 with ACN:MilliQ water (1:1; v:v) in all calibration solutions. Deuterated amino acids were used as internal standards. The dilution series in cell extract matrix was measured four times. The calibration functions were obtained by plotting peak area ratios versus concentrations of the $^{13}C,^{15}N$-isotopically labelled amino acids. Based on these functions, unweighted linear regression functions were constructed using the MultiQuant software. These calibration functions were used for the quantification of amino acids in treated HCE cell extracts taking the response factors (RF; see Suppl. Material for details) into account according to eq. 2 where a is the slope and b is the intercept of the calibration function of the $^{13}C,^{15}N$-isotopically labelled amino acids.

$$concentration_{Analyte} = \frac{[area_{Analyte}/area_{internal\ standard}] * RF - b}{a} \quad \text{(eq. 2)}$$

2.4.3. Validation

The validation process comprising intra-day and inter-day precision and accuracy as well as freeze-thaw stability measurements was carried out by measuring quality control (QC) samples. These, were prepared by spiking different amounts of ^{13}C,^{15}N-isotopically labelled amino acid mixture to untreated HCE cell extracts at different levels across the entire range. The deuterated amino acids 3,3,4,4,5,5,6,6-d8-L-Lys 2HCl (5 µg/mL), ring-d4-L-Tyr (250 ng/mL), and d8-L-Val (16 ng/mL) were used as internal standards. Eight different QC samples were prepared by dilution (1:12.5; 1:25; 1:100; 1:400; 1:800; 1:2000; 1:10 000 and 1:100 000) of the ^{13}C,^{15}N-isotopically labelled amino acids spiked HCE cell extracts with ACN:MilliQ water (1:1, v:v). The HCE cell extracts were finally diluted to 1:10 (% v/v) in all QC samples. The inter-day precision and accuracy were determined with n=8 at three different days within a week (day 1, 3, and 4) with a calibration series at the beginning and the end of the measurement sequence. Intra-day precisions and accuracies were calculated separately every single day.

The QC samples for the freeze-thaw stability test were frozen and thawed according to recommendations by the U.S. Food and Drug Administration (FDA) guidelines on bioanalytical method validation. The samples were measured four times and autosampler stability was verified on day four of the validation by measuring the calibration calibrants according to the FDA guidelines.

2.5. Data processing of untargeted analysis

Raw data (.wiff) files were converted to .abf files for using MS-Dial (version 2.80) with a combination of MassBank, MoNA, ReSpect, and GNPS databases. The MS-Dial software was used for peak alignment, peak detection, peak identification, and deconvolution [24,25]. The used parameters for MS-Dial are listed in detail in SI Table S4. Multivariate statistical evaluation of the preprocessed metabolic profiling data was performed with SIMCA-P+ (version12) (Umetrics, Umeå, Sweden). The signal intensity data were log transformed, scaled (Pareto), and finally a Partial least squares (PLS) analysis was carried out using log

EC_{50} values as the dependent (Y) variables and all the molecular features as X-variables. The heatmap was generated with Perseus and the data were scaled to z-score.

3. Results and discussion

3.1. Chromatographic conditions

Several common HILIC columns were screened initially and BEH Amide (1.7 µm) was finally selected for further optimization of the gradient profile, column temperature (30-60 °C), and flow rate (250-700 µL/min). The prime focus of these experiments was to achieve a separation of the amino acid pairs Leu/Ile, Asn/Asp, and Gln/Glu. Furthermore, the aim was to keep run times short at sufficient resolution of metabolites to reduce ion suppression (matrix) effects. A temperature of 40 °C and a flow rate of 300 µL/min were selected as a best compromise between a reasonable separation of the amino acids and good sensitivities (*i.e.*, better signal-to-noise, S/N). Figure 2 shows the MS/MS chromatograms (MS chromatogram in case of Gly) of the 20 proteinogenic amino acids obtained the with optimized HILIC method. The amino acids were widely spread over the chromatogram between 3 and 9 min. The isomeric amino acids leucine and isoleucine were fully separated, like the critical amino acid pairs Glu/Gln and Asn/Asp. Some peak tailing was observed for amino acids with basic side chains and aspartic acid. Such peak tailing can be reduced by using higher buffer concentrations at expense of signal intensity loss which was therefore not implemented.

3.2. Mass spectrometry settings and acquisition mode

The adopted acquisition mode should allow sensitive detection of the targeted compounds and, on the other hand, a molecular profiling without prior knowledge of the molecular structure of sample components. One option is to utilize product ion scans (termed MRM^{HR}) with unit mass Q1 precursor selection for fragmentation and HR-MS/MS spectra readout by the TOF mass analyzer. It allows comprehensive untargeted profiling in MS mode while additionally for preselected targets MS/MS spectra are recorded throughout the

chromatogram. Therefore, MS/MS chromatograms (EICs) can be generated for the targeted compounds. These EICs are benefiting from the effective filtering of the background noise and the narrow isolation windows (usually 5-10 mDa wide). Unfortunately, for untargeted molecules no MS/MS data are available if this acquisition mode is selected. This limits identification and metabolite coverage. Since DDA provides MS/MS spectra for the most abundant precursors only and does not allow to extract MS/MS-chromatograms, we decided to evaluate DIA with SWATH in comparison to MRM^{HR} (parameters see Suppl. Table S1) as data acquisition mode.

SWATH combines features of targeted and untargeted profiling assays. Each MS cycle in this acquisition mode consisted of a TOF MS scan over a predefined *m/z*, herein *m/z* 30-300, followed by a series of MS/MS experiments covering the entire m/z range by a set of sequential intermediate-sized Q1 precursor isolation windows (SWATH windows). Two distinct SWATH methods were compared: One with fixed SWATH windows which consisted of 27 MS/MS experiments each with 10 Da Q1 isolation width (SWATH with fixed Q1 windows; see SI Table S2 and SI Figure S1). A second method made use of variable Q1 precursor isolation windows which were narrower for the targeted precursors (*e.g.* 2-5 Da wide; one to four amino acids per SWATH window) and wider for other m/z ranges (SWATH with variable window approach; SWATH 2.0, see Table 1 and SI Figure S1). Co-eluting compounds which are co-isolated in the same SWATH window for fragmentation yield composite spectra. Hence, MS/MS spectra quality may be worse than in DDA, but deconvolution may remove contaminating ions leading to reasonable spectral quality. In the variable SWATH window approach, assay specificity can be adjusted by selection of narrow Q1 windows for targets. The great benefit of these SWATH methods is that MS/MS data are acquired comprehensively across the peak, over the entire chromatogram and across all samples. This enables post acquisition selection of the most suitable ion (precursor from MS^1, precursor from MS^2 if available, or any fragment ion from MS^2) for signal processing and data evaluation whichever is more selective and/or more sensitive. In this combined targeted/untargeted assay, ion source and fragmentation parameters were optimized for the

targeted amino acids (for MRM^{HR} method see SI Table S1, for SWATH with fixed Q1 windows approach see SI Table S2 and for the finally selected SWATH with variable Q1 windows approach, denoted SWATH 2.0, see Table 1). For each SWATH window CE and DP can be set individually to achieve the highest sensitivity for the target masses of interest.

The three acquisition modes mentioned above were compared to each other. The relative peak areas of the amino acid fragment masses having the same concentration were evaluated with MultiQuant software. The measured concentrations of the neat amino acid standard mixtures are listed in SI Table S3. The comparison in Figure S2, however, is based on the lowest measured concentration of each amino acid (*i.e.* concentration level 8), except for L-Cys (640 ng/mL), L-Asp (400 ng/mL), and L-Met (6.4 ng/mL). Figure S2 shows the results normalized to the peak areas of MRM^{HR}. The column chart clearly visualizes the sensitivity improvement of SWATH 2.0 (SWATH with variable Q1 windows) compared to SWATH (SWATH with fixed Q1 windows) and MRM^{HR}. Since most of the SWATH 2.0 windows contained only one target amino acid, the target-optimized CEs and DPs could be transferred from MRM^{HR} to the respective SWATH windows. In this context, it is interesting to note that, in spite of identical CE, DP, and accumulation times, the sensitivities of the SWATH method with variable windows was better than with MRM^{HR}. With fixed SWATH windows of 10 Da, a compromise in CE/DP had to be accepted for many amino acids because several of these targets were isolated in the same SWATH window (see SI Table S2) causing lower sensitivity. SWATH with variable Q1 windows was therefore selected as acquisition mode for the further work and MS settings optimized for each window.

With the optimized SWATH method (Table 1) peak group chromatograms, *i.e.,* series of overlapping MS/MS chromatograms as exemplified in Figure 3A, can be obtained for both targeted as well as untargeted metabolites due to comprehensive MS/MS data. The corresponding MS/MS spectra as measured in standard solution, HCE cell extract, and the deconvoluted MS/MS spectra with database match are shown in Figure 3B, 3C, and 3D, respectively. MS/MS spectra and peak group chromatograms of all the other target amino

acids are shown in SI Figure S3 and S4, respectively. MRM^{HR} offers this possibility only for the previously selected targets, but not for the untargeted metabolites. Examples of MS/MS chromatograms of untargeted metabolites are depicted in Figures 4A and 4B along with corresponding MS/MS spectra in standard solution, HCE extract and deconvoluted ones from HCE extract (Fig. 4C, 4D and 4E).

The most intensive signal (and/or the one with suitable assay specificity) was then selected post-acquisition for quantitative analysis of the targets (Table 2) while other signals were used as qualifiers for verification. Table 2 shows S/N ratios (calculated by PeakView software) for distinct EICs from a HCE cell extract measured using SWATH 2.0 (with variable Q1 windows). The S/N ratios are based on EICs for either the precursor ion in MS or MS/MS experiment or the fragment ion in the MS/MS experiment. As can be seen, the MS/MS signals are by far more sensitive (best S/N always obtained with fragment ion in the corresponding SWATH window except for Gly and Pro for which the precursor ion in the corresponding SWATH window gave higher S/N) (Table 2).

3.3. Method calibration and validation

Due to significant endogenic amino acid levels in HCE cells, no blank matrix was available for calibration and validation. Working with an artificial matrix or standard addition were ruled out as options. To ensure an accurate quantification, a surrogate calibration method was chosen [32]. In this approach, isotope-labelled standards were used as external calibrants instead of the authentic reference compounds. However, the detector response of the surrogate calibrant had to be the same as for the respective target analyte (parallelism of calibration lines). If a significant deviation occurs, as in this work for the target amino acids, a response factor correction (see SI, eq. S1) has to be applied. Response factors of uniformly-^{13}C,^{15}N-labelled amino acids were determined in comparison to authentic amino acids by their respective slope ratios (see SI Table S5) and applied to obtain corrected calibration functions (eq. 2) (SI Figure S5).

Matrix effects are a prime source for inaccurate results in quantitative LC-MS analysis with ESI and represent always a considerable challenge, especially in metabolomics [33]. Due to sample complexity and elimination of dedicated sample preparation to avoid metabolite losses, the accuracy of the results can be negatively influenced by the matrix effects. Therefore, matrix effects were estimated by establishing calibration series of surrogate calibrants (^{13}C,^{15}N-labelled amino acids) in matrix (HCE cell extract) and in matrix-free (neat) solutions using eq. 1. Table 3 summarizes the results for the determined matrix effects. For a majority of targeted amino acids, matrix effects are in an acceptable range. However, for a small number of targets, there is a significant matrix effects. Hence, it is advisable to perform matrix-matched calibration and for this reason a surrogate calibrant approach was selected.

Deuterated amino acids were used as internal standards (see Table 2). The calibration series consisted of 10 different concentrations of ^{13}C,^{15}N-amino acids spiked into untreated HCE cell extract samples. The linear range, lower-limit-of-quantification (LLOQ) and upper-limit-of-quantification (ULOQ) were determined according to FDA guidelines and these are summarized in Table 3 along with slope, intercept, and linearity values for each amino acid. These guidelines set the following criteria: the S/N ratio should be equal to 10 or higher with a precision of 20% and an accuracy of 100 ± 20% for the LLOQ and the ULOQ. The concentration levels should be in between the LLOQ and ULOQ and an accuracy of 100 ± 15% is needed. The linear range should cover two to three orders of magnitude with an R^2 of >0.99 for all analytes.

During the validation process intra-day and inter-day precision were determined with eight different QC samples, which were composed of ^{13}C,^{15}N-amino acids spiked into untreated HCE cell extract samples with deuterated amino acids as internal standards. Nevertheless, only three QC samples (QC_{low}, QC_{middle}, QC_{high}; for concentrations see SI Table S6) were taken into consideration for assessment. Accuracies (as % recoveries) and precisions (as coefficients of variation CV in %) were determined on three different days. All results were evaluated based on FDA guidelines with the following criteria: the QC samples should show

an accuracy of 100 ± 15 %. Every QC sample was measured eight times and according to the guidelines four out of the eight should be within 15% CV. Additionally, the freeze/thaw stability of the cell extracts was examined by preparing the same QC samples according to FDA guidelines.

The results of the validation and stability study are summarized in Table S6. Since accuracies were between 88 and 115% and precisions <13% CV, the targeted assay was found to be suitable for quantitative analysis of amino acids in HCE cell extracts.

3.4. Application to Human Corneal Epithelial Cell Extracts

The validity and applicability of the targeted assay was verified by measuring several HCE cell extracts (controls and IL treated ones) after 1:10 dilution. The sample injection order was randomized and is shown in Table S7. The corresponding quantitative results for amino acids are summarized in Table S8. The calculations of the concentrations were based on linear calibration functions of ^{13}C,^{15}N-isotopically labelled amino acids, taking the response factor correction into account (Table 3). Except for Cys, Gln, Asn, and Asp all proteinogenic amino acids were detected in the cell extracts.

A closer look at the amino acid concentrations as a function of the treatment with different ionic liquids (Table S8) reveals clear trends for the classification of the amino acids into the same chemical group. For example, the essential aliphatic amino acids Leu, Ile, and Val are not much affected by the addition of ionic liquids. Alanine concentrations in the IL-treated cells, on the other hand, decrease in comparison to the control samples depending on the toxicity of the IL. Similar to alanine, the concentration of glycine decreases the more toxic the IL is, except for the two choline-containing ILs. Altered concentrations are found for other amino acids as well. This supports the hypothesis of Ruokonen *et al.* that ILs, *e.g.* [Ch][Hex], interact with the cell membrane and affect the cell metabolism [4].

Additional information was provided by the untargeted metabolic profiling data. The data preprocessing was done with MS-Dial comprising peak spotting, deisotoping, adduct annotation, alignment, deconvolution, and identification based on metabolomics data bases

described in detail above [25]. Successful identification of several metabolites in HCE cell extracts by spectral match in various databases was verified with authentic standards (Table 4). The tentative metabolites were injected as a standard mixture dissolved in MilliQ water and product ion scans were acquired. Retention times and MS/MS spectra of the tentative metabolites acquired in the standard solution were compared with the corresponding data measured in the HCE cell extracts (Figure S6) and some representative results are shown in Figure 4. In case of acetylcholine and oxo-proline more than one peak with the same precursor mass was detected in the HCE extract, but the right peak was easily identified using the MS/MS spectra. Raw MS/MS spectra of SWATH acquisition often have poor spectral quality because they represent composite spectra of several precursors isolated in the same Q1 (SWATH) window which are fragmented simultaneously. The composite MS/MS spectra of the TOF-MS read out may be difficult to interpret in some cases. However, MS-DIAL has implemented a deconvolution tool which provides deconvoluted MS/MS spectra of good quality and matches them against database spectra. For example, the raw MS/MS spectrum of acetylcholine in the HCE extract (Figure 4D; top panel) is of relatively good quality and shows the three main fragments found in the reference spectrum of the standard solution (Figure 4C; top panel). Only a minor contaminating ion (m/z 103.9564) is present, which was, however, removed in the deconvoluted MS/MS spectrum (Figure 4E; top panel). On the other hand, the MS/MS spectrum of adenosine measured in the HCE extract shows poor quality (Figure 4D; middle panel). However, the deconvoluted spectrum perfectly matches with the MS/MS spectrum of the standard solution and database. The co-fragmented ions were successfully removed by the deconvolution approach. Hence, efficient deconvolution can overcome limited spectral quality of SWATH acquisition. Similarly, the MS/MS spectrum of pantothenic acid measured in the cell extract is not a good match with the spectrum obtained from the standard solution (Figure 4, bottom; *cf.* D and C). Again, the deconvolution process reestablishes an MS/MS spectrum of sufficient quality for spectral matching with standard solutions and MS/MS databases (Figure 4E, bottom).

PLS analysis was performed with EC_{50} values as dependent variables to explore whether there is a correlation between the metabolic profiles in IL-treated HCE cells and the toxicity of the ILs. Both data sets (Y and X-matrices) were log transformed prior to PLS. Figure 5 shows the resultant score plot of the first two principal components. The full statistical data of the PLS model is given in SI Table S9. The PLS model shows a good model fit ($R^2Y_{(cum)}$ = 0.997 with 4 principal components PCs) and yields a satisfactory predictive power ($Q^2_{(cum)}$ = 0.884 with 4 PCs). In the score plot the most toxic ionic liquids tributyl(tetradecyl)phosphonium acetate ([P_{14444}][OAc]) and tributyl(tetradecyl)phosphonium chloride ([P_{14444}]Cl) are grouped together in a cluster that is most distant from the controls. The second most toxic ILs tributylmethylphosphonium acetate ([P_{4441}][OAc]) and tributylmethylammonium acetate ([N_{4441}][OAc]) are also farther away from the controls than the least toxic IL 1,5-diazabicyclo(4,3,0)non-5-enium acetates ([DBNH][OAc]) and the reference compound *N*-methylmorpholine N-oxide (NMMO). The results are confirmed by the heatmap shown in Figure 6. It visualizes the relative concentration profiles of target amino acids and other identified metabolites according to the IL used for the treatment. Z-score normalization of the data was applied. The most significant perturbations can be seen for the two ILs with the highest toxicity ([P_{14444}][OAc] and [P_{14444}]Cl). Additionally, [P_{4441}][OAc] shows also significantly altered metabolite concentrations. This was partly expected regarding its EC_{50} value.

In general, our data suggest that cellular toxicometabolomics profiling of ILs can be a useful strategy to classify ILs for their toxicity potential. Already Ruokonen *et al.* pointed out that the used ILs can be separated into three groups based on their toxicity mechanism [4]. ILs, which exert toxicity by penetrating into the cell membrane ([P_{14444}][OAc], and [P_{14444}]Cl), ILs which affect both the cell membrane and the cell metabolism ([P_{4441}][OAc], and [Ch][Hexanoate]), and ILs which only influence cell metabolism ([N_{4441}][OAc], [emim][OAc], [DBNH][OAc], [Ch][OAc], and the reference compound NMMO) [4]. The different groups are also clearly seen in the LC-MS analysis results in form of grouped ILs in the PLS score plot (Figure 5). Therefore, the most harmful ILs are [P_{4441}][OAc], [P_{14444}][OAc], and [P_{14444}]Cl, however, there are two different toxicity mechanisms involved [4].

4. Conclusions

A targeted UHPLC-ESI-MS/MS method for amino acids combined with untargeted metabolic profiling in cells after IL treatment was developed and utilized for a preliminary toxicometabolomics study. Data independent acquisition using SWATH with variable Q1 window sizes (narrow Q1 precursor isolation windows for the target amino acids and wider Q1 windows for other metabolites) provided comprehensive MS and MS/MS data for quantification in either MS or MS/MS mode. The latter was shown to be more sensitive. Uniformly ^{13}C,^{15}N-labelled amino acids were used as surrogate calibrants for accurate quantification of the target metabolites. PLS analysis revealed a significant correlation between the toxicity (as measured by EC_{50} values) and the metabolic profiles in IL-treated HCE cells.

The results of the targeted and untargeted analysis support the data of Ruokonen *et al.* [4]. The most toxic ILs ($[P_{14444}][OAc]$ and $[P_{14444}]Cl$) result in different heatmap profiles compared to the practically harmless ILs (*e.g.* [emim][OAc]). Therefore, LC-MS based metabolic profiling is a useful strategy in the future for screening the toxicity of ILs. A full toxicometabolomics study will be carried out with selected ILs implementing a sufficient number of biological replicates and focusing on a wider metabolite coverage (positive and negative ion mode; hydrophilic and lipophilic metabolites) to allow derivation of meaningful interpretation of the toxicometabolic regulations.

Acknowledgements

ML is grateful for support of this work by the DAAD (German Academic Exchange Programme) project no. 5707 1060 and the Academy of Finland (project no. 276075).

References

[1] J.S. Wilkes, A short history of ionic liquids—from molten salts to neoteric solvents, Green Chem. 4 (2002) 73–80. doi:10.1039/b110838g.

[2] P. Sun, D.W. Armstrong, Ionic liquids in analytical chemistry, Anal. Chim. Acta. 661 (2010) 1–16. doi:10.1016/j.aca.2009.12.007.

[3] M. Cvjetko Bubalo, K. Radošević, I. Radojčić Redovniković, J. Halambek, V. Gaurina Srček, A brief overview of the potential environmental hazards of ionic liquids, Ecotoxicol. Environ. Saf. 99 (2014) 1–12. doi:10.1016/j.ecoenv.2013.10.019.

[4] S.-K. Ruokonen, C. Sanwald, A. Robciuc, S. Hietala, A.H. Rantamäki, J. Witos, A.W.T. King, M. Lämmerhofer, S.K. Wiedmer, Correlation between ionic liquid cytotoxicity and liposome-ionic liquid interactions, Chem. - A Eur. J. (2017). doi:10.1002/chem.201704924.

[5] X. Wang, C.A. Ohlin, Q. Lu, Z. Fei, J. Hu, P.J. Dyson, D.J. Gorman-Lewis, J.B. Fein, P. Stepnowski, W. Mrozik, J. Nichthauser, N. Gathergood, M.T. Garcia, P.J. Scammells, A.S. Wells, V.T. Coombe, K.M. Docherty, J.K. Dixon, C.F. Kulpa, F. Ganske, U.T. Bornscheuer, S.M. Lee, W.J. Chang, A.R. Choi, Y.M. Koo, J. Pernak, P. Chwala, J. Ranke, K. Molter, F. Stock, U. Bottin-Weber, J. Poczobutt, J. Hoffmann, B. Ondruschka, J. Filser, B. Jastorff, K.M. Docherty, C.F. Kulpa, M.T. Garcia, N. Gathergood, P.J. Scammells, E. Grabinska-Sota, J. Kalka, A. Latala, P. Stepnowski, M. Nedzi, W. Mrozik, R.P. Swatloski, J.D. Holbrey, S.B. Memon, G.A. Caldwell, K.A. Caldwell, R.D. Rogers, R.J. Bernot, E.E. Kennedy, G.A. Lamberti, C. Pretti, C. Chiappe, D. Pieraccini, M. Gregori, F. Abramo, G. Monni, L. Intorre, B. Jastorff, K. Molter, P. Behrend, U. Bottin-Weber, J. Filser, A. Heimers, B. Ondruschka, J. Ranke, M. Schaefer, H. Schroder, A. Stark, P. Stepnowski, F. Stock, R. Stormann, S. Stolte, U. Welz-Biermann, S. Ziegert, J. Thoming, P. Balczewski, B. Bachowska, T. Bialas, R. Biczak, W.M. Wieczorek, A. Balinska, S. Stolte, J. Arning, U. Bottin-Weber, M. Matzke, F. Stock, K. Thiele, M. Uerdingen, U. Welz-Biermann, B. Jastorff, J. Ranke, R.F.M. Frade, A. Matias, L.C. Branco, C.A.M. Afonso, C.M.M. Duarte, P. Stepnowski, A.C. Skladanowski, A. Ludwiczak, E. Laczynska, D.J. Couling, R.J. Bernot, K.M. Docherty, J.K. Dixon, E.J. Maginn, A. Cieniecka-Roslonkiewicz, J. Pernak, J. Kubis-Feder, A. Ramani, A.J. Robertson, K.R. Seddon, F. Stock, J. Hoffmann, J. Ranke, R. Stormann, B. Ondruschka, B. Jastorff, J. Ranke, A. Müller, U. Bottin-Weber, F. Stock, S. Stolte, J. Arning, R. Störmann, B. Jastorff, P. Stepnowski, P. Storoniak, D. Zhao, Y. Liao, Z. Zhang, P.H. V. Ewijk, J.A. Hoekstra, C. V. Rider, G.A. LeBlanc, C.A. Ohlin, P.J. Dyson, G. Laurenczy, A. Vidis, C.A. Ohlin, G. Laurenczy, E. Kusters, G. Sedelmeier, P.J. Dyson, M. Berridge, A. Tan, C. V. Rider, G.A. LeBlanc, J. Wu, T. Liu, J. Xie, F. Xin, L. Guo, T.J. Chen, J.Y. Jeng, C.W. Lin, C.Y. Wu, Y.C. Chen, N. Demaurex, D.P. Lew, K.-H. Kraus, G. Grynkiewicz, M. Poenie, R.Y. Tsien, Cytotoxicity of ionic liquids and precursor compounds towards human cell line HeLa, Green Chem. 9 (2007) 1191. doi:10.1039/b704503d.

[6] S. Pandey, Analytical applications of room-temperature ionic liquids: A review of recent efforts, Anal. Chim. Acta. 556 (2006) 38–45. doi:10.1016/j.aca.2005.06.038.

[7] N. Muhammad, Z. Man, M.A.B. Khalil, Ionic liquid-a future solvent for the enhanced uses of wood biomass, Eur. J. Wood Wood Prod. 70 (2012) 125–133. doi:10.1007/s00107-011-0526-2.

[8] P.C. Alves, D.O. Hartmann, O. Núñez, I. Martins, T.L. Gomes, H. Garcia, M.T. Galceran, R. Hampson, J.D. Becker, C.S. Pereira, Transcriptomic and metabolomic profiling of ionic liquid stimuli unveils enhanced secondary metabolism in Aspergillus

nidulans, BMC Genomics. 17 (2016) 1–18. doi:10.1186/s12864-016-2577-6.

[9] M.S.P. Boyles, C. Ranninger, R. Reischl, M. Rurik, R. Tessadri, O. Kohlbacher, A. Duschl, C.G. Huber, Copper oxide nanoparticle toxicity profiling using untargeted metabolomics, Part. Fibre Toxicol. 13 (2016) 1–20. doi:10.1186/s12989-016-0160-6.

[10] G. Hopfgartner, D. Tonoli, E. Varesio, High-resolution mass spectrometry for integrated qualitative and quantitative analysis of pharmaceuticals in biological matrices, Anal. Bioanal. Chem. 402 (2012) 2587–2596. doi:10.1007/s00216-011-5641-8.

[11] R. Bonner, G. Hopfgartner, SWATH acquisition mode for drug metabolism and metabolomics investigations, Bioanalysis. 8 (2016) 1735–1750. doi:10.4155/bio-2016-0141.

[12] B. Grund, L. Marvin, B. Rochat, Quantitative performance of a quadrupole-orbitrap-MS in targeted LC-MS determinations of small molecules, J. Pharm. Biomed. Anal. 124 (2016) 48–56. doi:10.1016/j.jpba.2016.02.025.

[13] A.T. Roemmelt, A.E. Steuer, T. Kraemer, Liquid chromatography, in combination with a quadrupole time-of-flight instrument, with sequential window acquisition of all theoretical fragment-ion spectra acquisition: validated quantification of 39 antidepressants in whole blood as part of a simultane, Anal Chem. 87 (2015) 9294–9301. doi:10.1021/acs.analchem.5b02031.

[14] D. Siegel, A.C. Meinema, H. Permentier, G. Hopfgartner, R. Bischoff, Integrated quantification and identification of aldehydes and ketones in biological samples, Anal. Chem. 86 (2014) 5089–5100. doi:10.1021/ac500810r.

[15] B. Drotleff, M. Hallschmid, M. Lämmerhofer, Quantification of steroid hormones in plasma using a surrogate calibrant approach and UHPLC-ESI-QTOF-MS/MS with SWATH-acquisition combined with untargeted profiling, Anal. Chim. Acta. (2018) 1–11. doi:10.1016/j.aca.2018.03.040.

[16] M. Schwaiger, E. Rampler, G. Hermann, W. Miklos, W. Berger, G. Koellensperger, Anion-Exchange Chromatography Coupled to High-Resolution Mass Spectrometry: A Powerful Tool for Merging Targeted and Non-targeted Metabolomics, Anal. Chem. 89 (2017) 7667–7674. doi:10.1021/acs.analchem.7b01624.

[17] Y. Zhang, A. Bilbao, T. Bruderer, J. Luban, C. Strambio-de-castillia, E. Varesio, The Use of Variable Q1 Isolation Windows Improves Selectivity in LC-SWATH-MS Akquisition, 14 (2015) 4359–4371. doi:10.1021/acs.jproteome.5b00543.

[18] A.T. Roemmelt, A.E. Steuer, M. Poetzsch, T. Kraemer, Liquid chromatography, in combination with a quadrupole time-of-flight instrument (LC QTOF), with sequential window acquisition of all theoretical fragment-ion spectra (SWATH) acquisition: systematic studies on its use for screenings in clinical and foren, Anal Chem. 86 (2014) 11742–11749. doi:10.1021/ac503144p.

[19] N.S. Greenspan, A.K. Sheth, V. Desai, HIV vaccine development and broadly neutralizing antibodies, Evol. Med. Public Heal. 2015 (2015) 75–75. doi:10.1021/acs.analchem.8b02377.

[20] J. Zhou, Y. Li, X. Chen, L. Zhong, Y. Yin, Development of data-independent acquisition workflows for metabolomic analysis on a quadrupole-orbitrap platform, Talanta. 164 (2017) 128–136. doi:10.1016/j.talanta.2016.11.048.

[21] R. Bonner, G. Hopfgartner, SWATH data independent acquisition mass spectrometry

for metabolomics, TrAC - Trends Anal. Chem. (2018). doi:10.1016/j.trac.2018.10.014.

[22] G. Hopfgartner, D. Tonoli, E. Varesio, High-resolution mass spectrometry for integrated qualitative and quantitative analysis of pharmaceuticals in biological matrices, Anal. Bioanal. Chem. 402 (2012) 2587–2596. doi:10.1007/s00216-011-5641-8.

[23] J.D. Venable, M.-Q. Dong, J. Wohlschlegel, A. Dillin, J.R. Yates, Automated approach for quantitative analysis of complex peptide mixtures from tandem mass spectra, Nat. Methods. 1 (2004) 39–45. doi:10.1038/nmeth705.

[24] J. Ji, P. Zhu, F. Cui, F. Pi, Y. Zhang, X. Sun, The disorder metabolic profiling in kidney and spleen of mice induced by mycotoxins deoxynivalenol through gas chromatography mass spectrometry, Chemosphere. 180 (2017) 267–274. doi:10.1016/j.chemosphere.2017.03.129.

[25] H. Tsugawa, T. Cajka, T. Kind, Y. Ma, B. Higgins, K. Ikeda, M. Kanazawa, J. Vandergheynst, O. Fiehn, M. Arita, MS-DIAL: Data-independent MS/MS deconvolution for comprehensive metabolome analysis, Nat. Methods. 12 (2015) 523–526. doi:10.1038/nmeth.3393.

[26] S. Salihovic, T. Fall, A. Ganna, C.D. Broeckling, J.E. Prenni, T. Hyötyläinen, A. Kärrman, P.M. Lind, E. Ingelsson, L. Lind, Identification of metabolic profiles associated with human exposure to perfluoroalkyl substances, J. Expo. Sci. Environ. Epidemiol. (2018). doi:10.1038/s41370-018-0060-y.

[27] S. Guo, J.A. Duan, D. Qian, Y. Tang, Y. Qian, D. Wu, S. Su, E. Shang, Rapid determination of amino acids in fruits of Ziziphus jujuba by hydrophilic interaction ultra-high-performance liquid chromatography coupled with triple-quadrupole mass spectrometry, J Agric Food Chem. 61 (2013) 2709–2719. doi:10.1021/jf305497r.

[28] M. Dell'mour, L. Jaitz, E. Oburger, M. Puschenreiter, G. Koellensperger, S. Hann, Hydrophilic interaction LC combined with electrospray MS for highly sensitive analysis of underivatized amino acids in rhizosphere research, J Sep Sci. 33 (2010) 911–922. doi:10.1002/jssc.200900743.

[29] M.A. Alterman, Amino Acid Analysis : Methods and Protocols, Humana Press, Totowa, NJ, 2012. doi:10.1007/978-1-61779-445-2.

[30] G. Sharma, S.V. Attri, B. Behra, S. Bhisikar, P. Kumar, M. Tageja, S. Sharda, P. Singhi, S. Singhi, Analysis of 26 amino acids in human plasma by HPLC using AQC as derivatizing agent and its application in metabolic laboratory, Amino Acids. 46 (2014) 1253–1263. doi:10.1007/s00726-014-1682-6.

[31] K. Araki-Sasaki, Y. Ohashi, T. Sasabe, K. Hayashi, H. Watanabe, Y. Tano, H. Handa, An SV40-immortalized human corneal epithelial cell line and its characterization, Invest. Ophthalmol. Vis. Sci. 36 (1995) 614–621. http://dx.doi.org/.

[32] W. Li, L.H. Cohen, Quantitation of Endogenous Analytes in Biofluid without a True Blank Matrix, Anal. Chem. 75 (2003) 5854–5859. doi:10.1021/ac034505u.

[33] S. Schiesel, M. Lämmerhofer, W. Lindner, Multitarget quantitative metabolic profiling of hydrophilic metabolites in fermentation broths of β-lactam antibiotics production by HILIC–ESI–MS/MS, Anal. Bioanal. Chem. 396 (2010) 1655–1679. doi:10.1007/s00216-009-3432-2.

Figure 1: Used ionic liquids (ILs) with corresponding *concentrations* used for IL treatment; Molar mass of the IL and EC_{50}-value ± STD

Figure 2: Chromatographic separation of a standard solution of 20 proteinogenic amino acids in HILIC mode using a BEH Amide column (10 µg/mL) and the optimized SWATH 2.0 method. The m/z values of precursor and fragment ions (bold) are listed on the right side. For the EIC chromatograms fragment masses were used.

Figure 3: Targeted analysis of Tryptophan (precursor: m/z 205.097 and main fragment: m/z 146.060) in HCE cell extracts (QC sample). (A) Peak group chromatograms measured by SWATH 2.0, the extracted fragment mass was m/z 146.06 with an extraction window of +/- 5 mDa; (B) MS/MS spectrum by SWATH 2.0 measured in HCE cell extracts; (C) MS/MS spectrum of tryptophan in neat standard solution measured by MRM^{HR}; (D) deconvoluted MS/MS spectrum (blue) matched against database spectrum (red).

Figure 4: Examples of identified metabolites from untargeted analysis of HCE cell extracts. (A) EIC MS/MS chromatogram (Acetylcholine: m/z 146.1153, Adenosine: m/z 268.1030 and Pantothenic acid: m/z 220.1168; m/z values were used for EIC generation in A and B) of standard solution with an extraction window of +/- 5 mDa; (B) EIC MS/MS chromatogram of HCE extract with an extraction window of +/- 5 mDa; (C) MS/MS spectrum from standard solution; (D) MS/MS spectrum from HCE extract; (E) deconvoluted MS/MS spectrum from the HCE extract (blue) matched against database spectrum (red).

Figure 5: Multivariate data analysis (PLS) showing the correlation of toxicity data (log EC_{50} as dependent variable) and metabolic profile (all molecular features log transformed as independent variables): Score plot of 1^{st} and 2^{nd} principal component (for statistical parameters see SI Table S9).

Figure 6: Heatmap showing perturbations of identified features by ILs as compared to untreated controls of HCE cells; intensities were z-score normalized and the samples (treated with IL) are sorted by EC_{50} values (from low on top to high at the bottom).

Table 1: Overview of the MS-settings used for SWATH acquisition mode with variable Q1 window widths; in bold are the "targeted" Q1 windows

Experiment number	Q1 window range [m/z]	target amino acid; precursor mass [m/z]; fragment mass [m/z]	Collision energy [V]	Declustering potential [V]
		SWATH with variable Q1 window width		
0	30 - 1000	TOF MS	10	30
1	30 - 75		10	20
2	**75 - 80**	Gly; 76.0393; -	5	20
3	80 - 89		10	20
4	**89 - 95**	Ala;90.0547;44.0533	21	10
5	95 - 105		10	20
6	**105 - 111**	Ser;106.0499;60.0462	20	10
7	111 - 115		10	30
8	**115 - 117**	Pro;116.0706;70.0685	20	20
9	**117 - 119**	Val;118.0863;72.0833	16	20
10	**119 - 121**	Thr;120.0655;74.0618	17	30
11	**121 - 123**	Cys;122.0270;76.0236	20	20
12	123 - 131	Leu/Ile;132.1019;86.0979	17	30
13	**131 - 135**	Asn;133.0608;74.0258 Asp;134.0448;74.0260	12	30
14	135 - 146	Gln;147.0764;84.0457	14	30
15	**146 - 149**	Lys;147.1128;84.0822 Glu;148.0613;84.0450	23	15
16	**149 - 151**	Met;150.0583;104.0530	15	60
17	151 - 155		25	20
18	**155 - 157**	His;156.0768;110.0710	21	40
19	157 - 164		10	30
20	**164 - 167**	Phe;166.0863;120.0810	23	15
21	167 - 174		23	15
22	**174 - 177**	Arg;175.1190;70.0679	35	50
23	177 - 181		21	10
24	**181 - 183**	Tyr;182.0812;136.0752	22	20
25	183 - 204		30	30
26	**204 - 206**	Trp;205.0972;146.0598	25	10
27	206 - 300		25	10

Table 2: Comparison of S/N ratios (as calculated with PeakView) for EICs of precursor ions from TOF-MS scans, of precursor ions from MS/MS experiment (i.e. corresponding SWATH window), and of fragment ions from MS/MS experiment (SWATH window) as measured in HCE cell extract (QC sample)

			Signal-to-noise			
Amino acid	Precursor ion [m/z]	Fragment ion [m/z]	Internal standard[b]	S/N Precursor TOF-MS	S/N Precursor SWATH window	S/N Fragment SWATH window
Gly	76.0393	-	d-Tyr	43	**1407**	-
L-Ala	90.0547	44.0533	d-Tyr	175	13	**418**
L-Ser	106.0499	60.0462	d-Tyr	33	10	**184**
L-Pro[c]	116.0706	70.0685	d-Tyr	2962	**5286**	3439
L-Val	118.0863	72.0800	d-Val	224	336	**1069**
L-Thr	120.0655	74.0618	d-Tyr	379	215	**1819**
L-Cys	122.0270	76.0236	d-Tyr	-[a]	-[a]	-[a]
L-Leu	132.1019	86.0979	d-Val	133	114	**1232**
L-Ile	132.1019	86.0979/(69.0727)	d-Val	122	140	**2671/(111)**
L-Asn	133.0608	88.0395	d-Tyr	-[a]	-[a]	-[a]
L-Asp	134.0448	88.0394	d-Lys	-[a]	-[a]	-[a]
L-Gln	147.0764	84.0457	d-Tyr	-[a]	-[a]	-[a]
L-Lys	147.1128	84.0822	d-Lys	46	6	**297**
L-Glu	148.0613	84.0450	d-Tyr	246	36	**1017**
L-Met	150.0583	104.0527	d-Val	297	292	**971**
L-His	156.0768	110.0714	d-Lys	111	90	**849**
L-Phe	166.0863	120.0814	d-Val	592	96	**6762**
L-Arg	175.1190	70.0679	d-Lys	200	-	**1108**
L-Tyr	182.0812	136.0752	d-Tyr	318	41	**1579**
L-Trp	205.0972	146.0598	d-Val	43	-	**645**

[a] not detected in HCE cell extract samples
[b] assignment based on retention times of the amino acid and the corresponding internal standard
[c] very high abundant in HCE cell extracts, therefore end of linear range (ULOQ) is easily reached
in bold: most sensitive signal with highest S/N ratio used for quantitation (except Pro for which also the fragment ion was used)

Table 3: Summary of calibration, method sensitivity and estimation of matrix effects (n = 4)

Compound Name	M [g/mol]	t_R [min]	Product ion (m/z)	Slope	S_e (slope)	Intercept	S_e (intercept)	Linearity (R^2)	LLOQ [ng/mL]	ULOQ [µg/mL]	Absolute matrix effect [%]
Glycine	79.0	5.24	79.04	0.00442	0.00010	-0.05	0.72	0.9943	47	19	122
L-Alanine	94.1	4.74	47.05	0.00527	0.00005	-0.11	0.26	0.9990	56	11	107
L-Serine	110.1	5.72	63.05	0.00449	0.00005	-0.30	0.28	0.9989	66	13	99
L-Proline	122.1	3.83	75.08	0.15950	0.00105	0.14	0.22	0.9996	1	0.5	72
L-Valine	124.1	3.78	77.09	0.04902	0.00049	0.08	0.33	0.9988	1	1.8	76
L-Threonine	125.1	5.09	78.07	0.00852	0.00008	0.00	0.26	0.9991	19	7.5	100
L-Cysteine[a]	126.0	9.11	124.02	0.00027	0.00000	0.20	0.03	0.9998	600	60	145
L-Leucine	139.1	3.18	92.11	0.07897	0.00103	-0.12	0.94	0.9983	5	2	90
L-Isoleucine	139.1	3.36	92.11	0.09605	0.00054	-0.03	0.46	0.9997	5	2	105
L-Aspartic acid	139.1	6.85	92.05	0.00071	0.00001	0.02	0.08	0.9995	333	33	152
L-Lysine	155.1	8.15	90.10	0.00580	0.00003	0.09	0.03	0.9998	6	2.3	105
L-Glutamic acid	154.1	5.63	89.06	0.00942	0.00016	-0.32	1.31	0.9971	92	18.4	134
L-Methionine	156.1	3.60	109.06	0.01078	0.00021	-0.07	0.76	0.9968	23	9.3	78
L-Histidine	165.1	8.12	118.08	0.02213	0.00034	0.57	0.40	0.9980	24	2.4	110
L-Phenylalanine	176.1	3.15	129.11	0.04264	0.00056	0.03	0.62	0.9982	2	2.6	80
L-Arginine	185.1	7.86	75.08	0.01401	0.00010	0.16	0.14	0.9995	2	3.3	120
L-Tyrosine	192.1	4.00	145.10	0.00572	0.00005	0.09	0.41	0.9992	28	22.7	85

$^{13}C,^{15}N$ isotopically labelled amino acids (Eurisotop Std) were used as surrogate calibrants

The linear range is from LLOQ to ULOQ

The amino acids Trp, Asn and Gln were not included in the $^{13}C,^{15}N$ isotopically labelled amino acid standard mixture. Asn and Gln were therefore not calibrated but were also not detected in the HCE cell extracts at all. Trp was calibrated based on $^{13}C,^{15}N$-Lys as surrogate calibrant (see Table S5)

[a] Cysteine was detected as the dimer cystine with m/z 124.02 in the SWATH window of m/z 206 - 300

Table 4: Identified metabolites from untargeted profiling in HCE extracts (other than amino acids)

Compound	sum formula	t_R in neat solution [min]	t_R in HCE extracts [min]	Δt_R [min]	Precursor m/z (experimental)	Precursor m/z (calculated)	error [ppm]	Fragment masses [m/z]
Acetylcholine	$C_7H_{16}NO_2$	1.69	1.66	0.03	146.1177	146.1176	0.7	87.0454; 60.0836
Adenosine	$C_{10}H_{13}N_5O_4$	2.00	1.98	0.02	268.1041	268.1040	0.4	136.0626
Betaine	$C_5H_{11}NO_2$	3.33	3.31	0.02	118.0866	118.0863	2.5	59.0756; 58.0679
Choline	$C_5H_{14}NO$	2.26	2.18	0.08	104.1071	104.1070	1.0	60.0837
D-(+)-Pantothenic acid	$C_9H_{17}NO_5$	1.23	1.21	0.02	220.1178	220.1180	0.9	202.1086; 184.0982; 116.0358; 90.0571
Guanosine	$C_{10}H_{13}N_5O_5$	3.32	3.31	0.01	284.1006	284.0990	5.6	152.057
L-5-Oxoproline	$C_5H_7NO_3$	2.80	2.75	0.05	130.0497	130.0499	1.5	84.0463; 56.0531
O-Acetyl-L-carnitine	$C_9H_{17}NO_4$	2.92	2.94	-0.02	204.1229	204.1230	0.5	145.0496; 85.0295; 60.0832
Taurine	$C_2H_7NO_3S$	3.91	3.86	0.05	126.0212	126.0219	5.6	108.0125; 44.0551
Thiamine	$C_{12}H_{17}N_4OS$	3.59	3.51	0.08	265.1115	265.1118	1.1	144.0479; 122.0722; 81.0465
Norvaline	$C_5H_{11}NO_2$	3.29	3.31	-0.02	118.0858	118.0863	4.2	101.0609; 100.0770; 83.0508; 59.0755; 58.0684; 56.0530; 55.0579
5-Aminopentanoic acid	$C_5H_{11}NO_2$	3.29	3.31	-0.02	118.0858	118.0863	4.2	101.0609; 100.0770; 83.0508; 59.0755; 58.0684; 56.0530; 55.0579

[HMDB]: Human metabolome database

NMMO

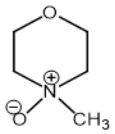

117.15 g/mol
250 mM
295 ± 11 mM

[DBNH][OAc]

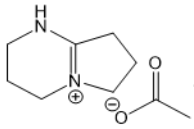

184.20 g/mol
65 mM
69 ± 11 mM

[Ch][OAc]

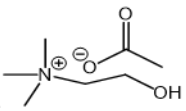

163.21 g/mol
60 mM
55 ± 9 mM

[emim][OAc]

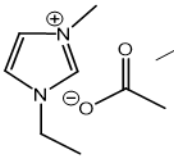

170.21 g/mol
48 mM
46 ± 9.3 mM

[Ch][Hex]

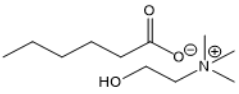

219.32 g/mol
9 mM
16 ± 3.7 mM

[P_{4441}][OAc]

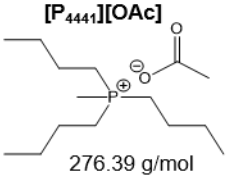

276.39 g/mol
12 mM
10 ± 1.3 mM

[N_{4441}][OAc]

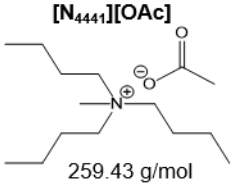

259.43 g/mol
15 mM
9.8 ± 0.7 mM

[P_{14444}][OAc]

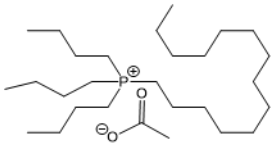

458.70 g/mol
0.01 mM
0.0071 ± 0.0005 mM

[P_{14444}]Cl^-

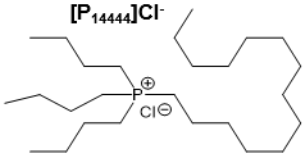

435.20 g/mol
0.01 mM
0.0041 ± 0.0006 mM

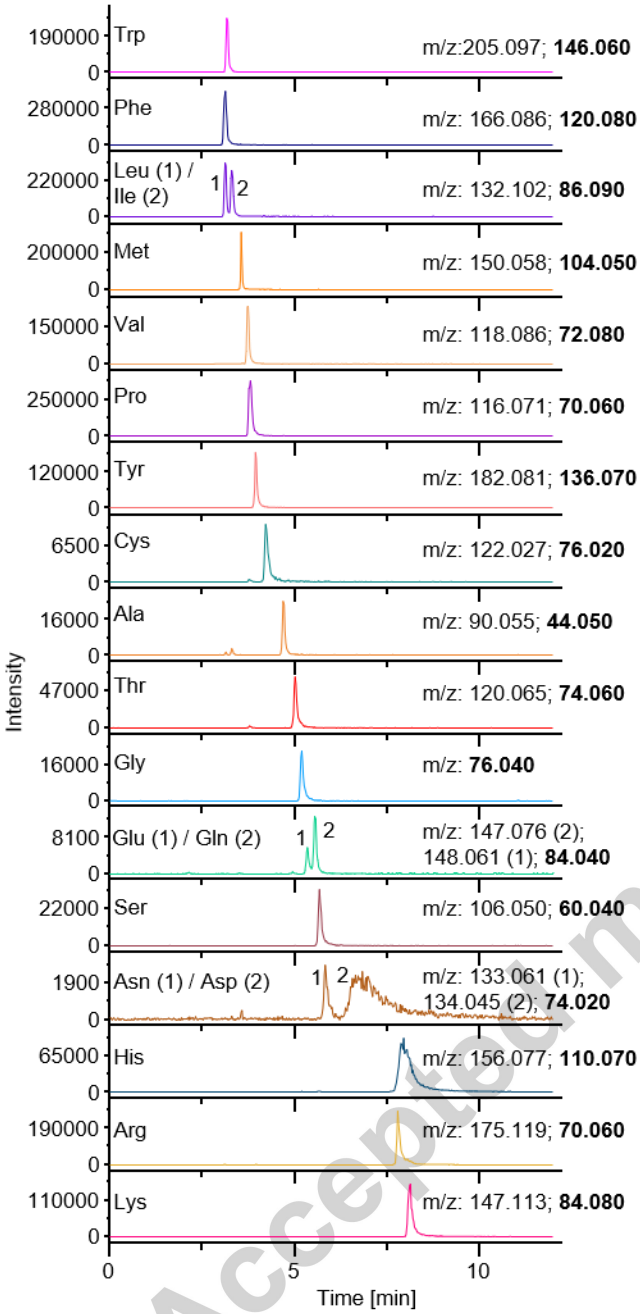

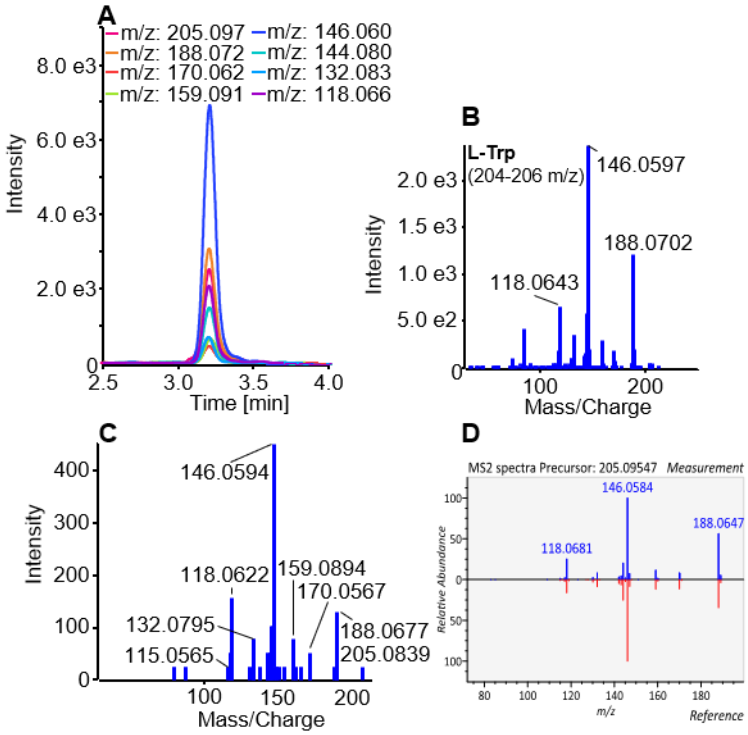

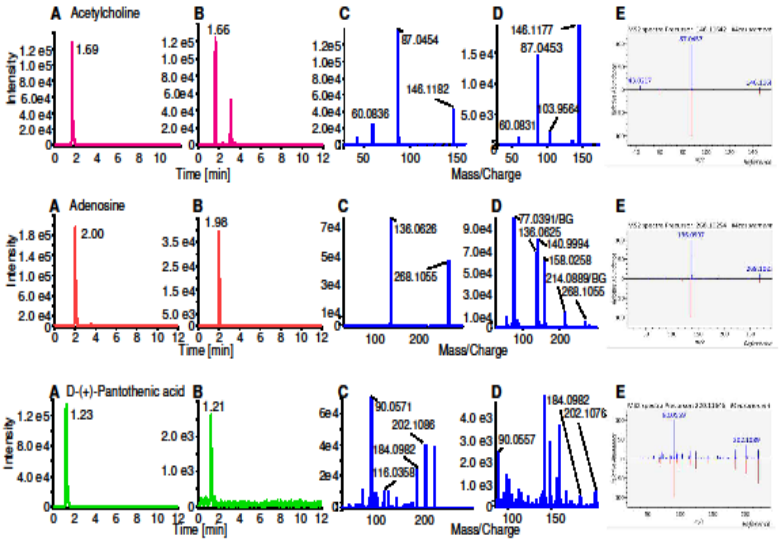
A Acetylcholine
1.69
B
1.66
C
87.0454
146.1182
60.0836
D
146.1177
87.0453
103.9564
60.0831
E
Intensity
Time [min]
Mass/Charge
A Adenosine
2.00
B
1.98
C
136.0626
268.1055
D
77.0391/BG
136.0625
140.9994
158.0258
214.0899/BG
268.1055
E
Intensity
Time [min]
Mass/Charge
A D-(+)-Pantothenic acid
1.23
B
1.21
C
90.0571
202.1086
184.0982
116.0358
D
184.0982
202.1076
90.0557
E
Intensity
Time [min]
Mass/Charge

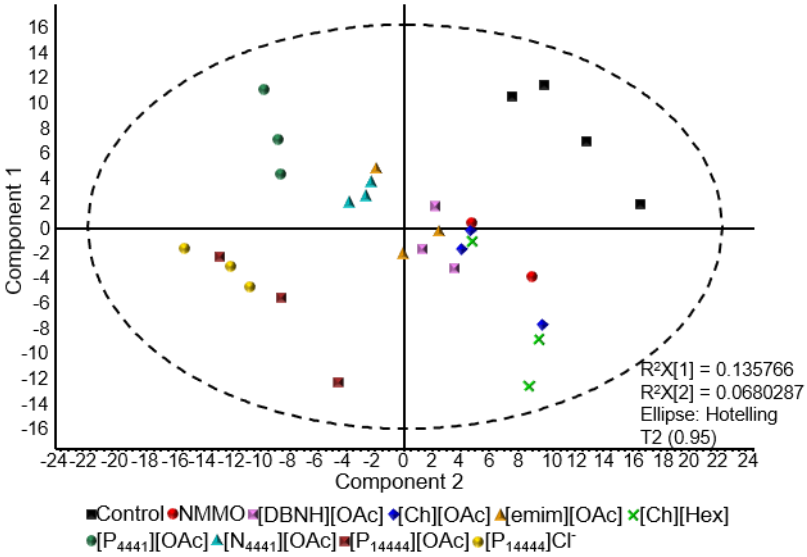

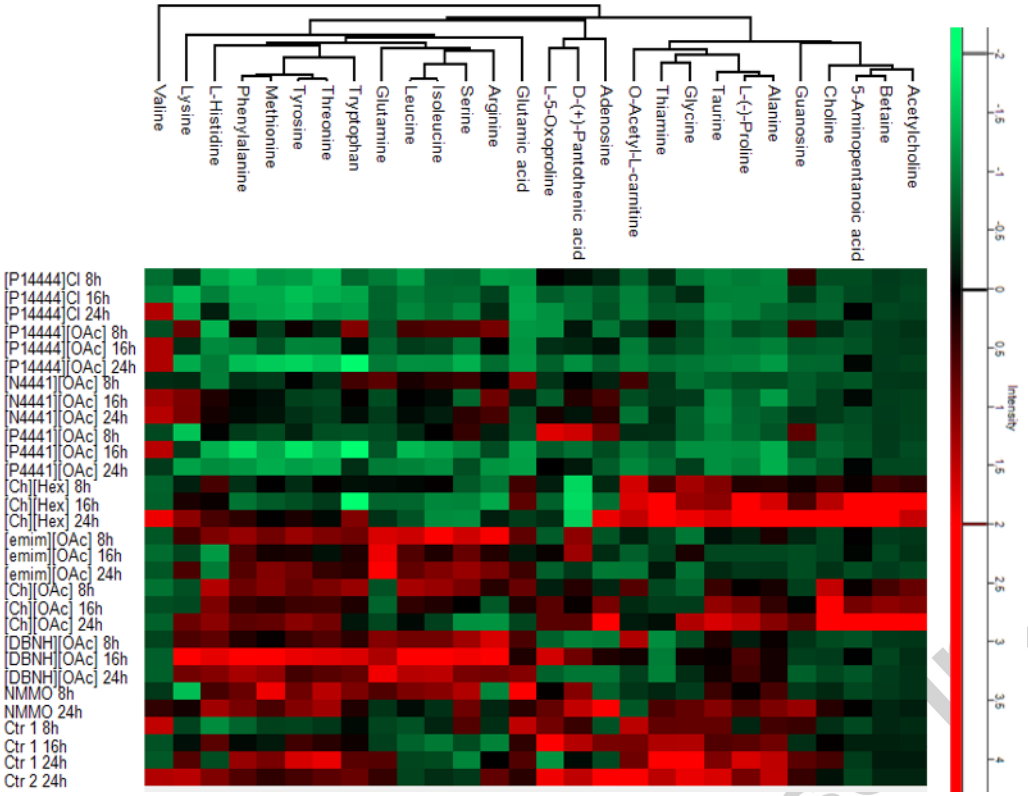

Highlights

- UHPLC-ESI-MS/MS method for quantitative amino acids analysis in cells developed
- Data-independent acquisition allows simultaneous untargeted metabolic profiling
- PLS reveals a correlation between metabolic profiles and toxicity of ILs
- The most toxic ILs tested were $[P_{4441}][OAc]$, $[P_{14444}][OAc]$ and $[P_{14444}]Cl$
- LC-MS metabolic profiling seems to be a useful strategy to classify the toxicity of ILs